Formation of InAs/GaAs quantum dots from a subcritical InAs wetting layer: A reflection high-energy electron diffraction and theoretical study

H. Z. Song and T. Usuki
Nanotechnology Research Center, Fujitsu Lab. Ltd., Morinosato-Wakamiya 10-1, Atsugi, Kanagawa 243-0197, Japan and CREST, Japan Science and Technology Agency, Kawaguchi 332-0012, Japan

Y. Nakata and N. Yokoyama
Nanotechnology Research Center, Fujitsu Lab. Ltd., Morinosato-Wakamiya 10-1, Atsugi, Kanagawa 243-0197, Japan

H. Sasakura and S. Muto
Department of Applied Physics, Hokkaido University, Sapporo 060-8628, Japan, and CREST, Japan Science and Technology Agency, Kawaguchi 332-0012, Japan

(Received 28 July 2005; revised manuscript received 18 November 2005; published 20 March 2006)

InAs/GaAs quantum dots (QD's) are formed by postgrowth annealing of an InAs wetting layer thinner than the critical thickness for the transition from two- (2D) to three-dimensional (3D) growth mode. Reflection high energy electron diffraction is used to monitor the QD formation. Based on a mean-field theory [Phys. Rev. Lett. **79**, 897 (1997)], the time evolution of total QD's volume, first increasing and finally saturating, is well explained by precursors forming during wetting layer growth and converting into nucleated QD's after growth stop. Both the saturation QD's volume and the QD nucleation rate depend exponentially on the InAs coverage. These behaviors and their temperature and InAs growth rate dependences are essentially understandable in the frame of the mean-field theory. Similar analysis to conventional QD growth suggests that the often observed significant mass transport from wetting layer to QD's can be ascribed to the precursors existing before 2D-3D growth mode transition.

DOI: 10.1103/PhysRevB.73.115327 PACS number(s): 68.65.Hb, 68.35.Bs, 61.14.Hg

I. INTRODUCTION

The formation of self-assembled semiconductor quantum dots (QD's) has received significant attention due to the interesting properties of QD's and their prospects in optoelectronic device applications.[1] However, the exact mechanisms in the self-assembly have not been well understood yet, although considerable effort has been devoted.[2,3] It is considered that there are two possibilities: consuming the adatoms on the wetting layer and directly consuming the wetting layer.[4] In conventional QD growth, these two processes are mixed together and may interact with each other since the deposition continues after the transition from two—(2D) to three-dimensional (3D) growth mode. It makes the dynamics of QD formation complicated and the analysis difficult. Experimental studies of QD formation without deposition flux is thus required[5] to enable a separated study of wetting layer consumption in QD formation process. QD's formed from a wetting layer thinner than the critical thickness for conventional 2D-3D growth mode transition has been studied in Ge/Si system,[6] but such studies on III-V compounds,[7] especially quantitative investigations, are still lacking.

In the experimental studies of self-assembled QD's, atomic-force microscope (AFM) and scanning tunneling microscope (STM) are the main techniques for characterizing the QD formation process, but it is difficult to use them as a real-time monitor. In addition, as has been pointed out,[8] the cooling down procedure, which is necessary before analysis of AFM or STM, is rather effective in changing the surface morphology to be far from the original. As a matter of fact, the usually used reflection high energy electron diffraction (RHEED) is the most convenient way of real-time monitoring of QD formation, as has been widely reported.[9–11] Accordingly, we use RHEED as the main tool of analyzing the QD formation in this work.

On GaAs substrates, here we investigate the progression of an InAs wetting layer thinner than but close to the critical thickness for 2D-3D transition, which is thus termed "subcritical" hereafter. Lower density of InAs/GaAs QD's are found to form during the postgrowth annealing. The QD formation process is quantitatively analyzed by real-time RHEED. The results are explained in view of precursors formed during InAs wetting layer growth and transforming into QD's following the growth stop. The role of precursors in conventional QD formation is also discussed.

II. EXPERIMENTAL RESULTS

Our samples were fabricated by molecular beam epitaxy on semi-insulating GaAs (001) substrates. InAs was deposited on a buffer layer of GaAs. Following the stop of InAs deposition, a period of postgrowth annealing was performed without changing the substrate temperature and the arsenic pressure.

The changes in QD's with varying conditions are firstly examined by AFM measurements. To obtain images reflecting the as-formed QD's, the sample holder is suddenly cooled down by switching off the substrate heater and then taken off the heater within 20 s. We do not use samples with postgrowth annealing time less than 40 s for AFM observa-

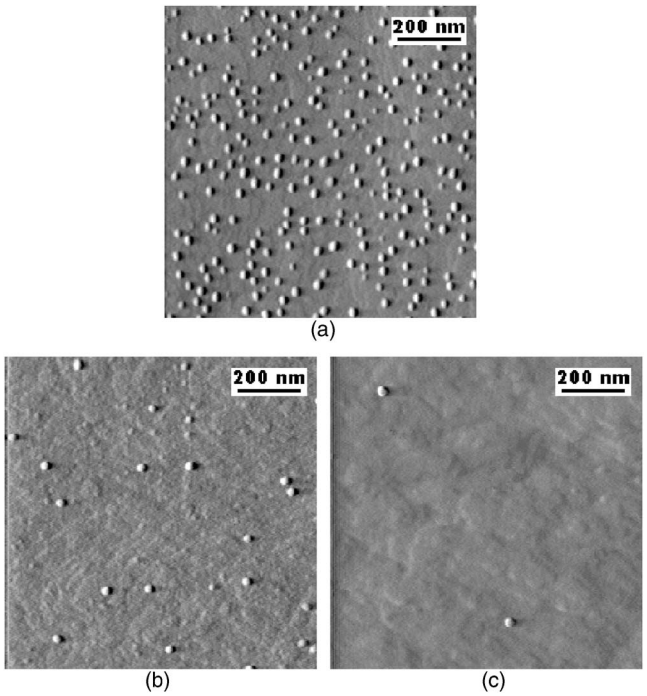

FIG. 1. AFM images of InAs/GaAs QD's formed by 60 s of postgrowth annealing after depositing (a) 1.69, (b) 1.55, and (c) 1.49 ML of InAs at 480 °C with a growth rate of 0.031 ML/s.

tion because the morphology may be still changing during the cooling down process. In our experimental system, at 480 °C and with InAs growth rate of 0.031 monolayers (ML) per second, the nominal critical InAs wetting layer thickness for 2D-3D growth mode transition is 1.66 ML. Figure 1(a) shows the AFM image of a QD sample conventionally grown by depositing 1.69 ML of InAs followed by 60 s of postgrowth annealing. It has a QD number density of 2.2×10^{10} cm^{-2}. If we stop depositing InAs before 2D-3D transition, postgrowth annealing of such a subcritical wetting layer also gives rise to finite density of QD's. As shown in Figs. 1(b) and 1(c) for 60 s of annealing, InAs coverage of 1.55 ML produces a QD ensemble with density of 2.0×10^{9} cm^{-2}, and a small decrease of coverage down to 1.49 ML leads to one order of magnitude lower QD density, 1.6×10^{8} cm^{-2}. The size of the QD's for these conditions are not very different.

Real-time RHEED is used to monitor the process of QD formation in detail. During the growth and postgrowth annealing, the substrate was fixed to observe the RHEED image along the [100] azimuth. The insets in Fig. 2 show typical RHEED images before, at the beginning of and after the QD formation. The monitored area is selected to be corresponding to one of the brightest spots after QD formation, as indicated by the rectangular marks in the inset images. The integrated RHEED intensity in the marked area was recorded with the scanning time, as shown in Fig. 2, in which the points corresponding to the inset images are indicated by arrows. Since RHEED intensity is proportionally correlated with the total QD's volume, we use the RHEED intensity recorded in the way shown in Fig. 2 as a measure of total QD's volume in this work.

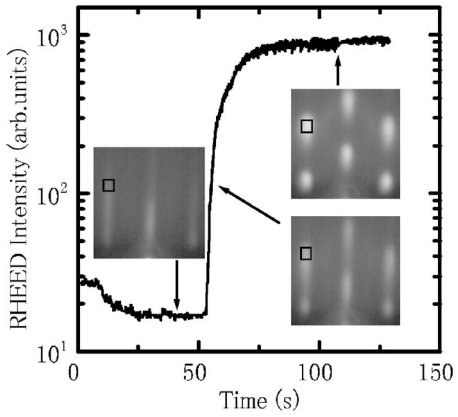

FIG. 2. A representative time-scanned RHEED intensity curve. The insets show typical RHEED images before, at the beginning of, and after the formation of QD's. The RHEED intensity is taken by integrating over the marked area in the images. The intensity of RHEED images is logarithmically scaled.

In Fig. 3(a), scattered symbols demonstrate a series of time-scanned RHEED intensity for InAs/GaAs QD formation at 480 °C with different coverage of InAs deposited at 0.031 ML/s. For the sake of clarity, the zero point of the

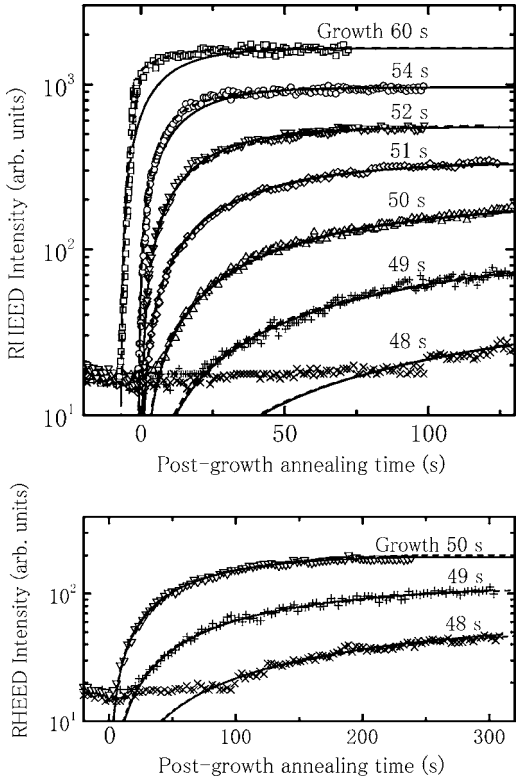

FIG. 3. RHEED intensity evolution with postgrowth annealing for InAs deposited with a rate $F=0.031$ ML/s at 480 °C. The scattered symbols are experimental data. The solid curves are the fitted results according to Eq. (1) and the dashed lines are the simulation using Eqs. (3) and (4) by setting the initial conditions: $t=t_0=43$ s, $n_1(t_0)=0.03$ ML, $n_2(t_0)=0.0006$ ML, $n_3(t_0)=0$, $D\sigma_2=20$, $D\sigma_3=40$, $\gamma_0=0.089$ s^{-1}, $E(F=0)=2.1$ eV, and $E(F=0.031)=21$ eV. The results for longer annealing times are shown in (b).

time axis is taken to be the stop of InAs growth rather than the beginning of InAs deposition such as in Fig. 2. The onsets of rapid increase for 60 and 54 s of InAs deposition, occur 7 s and 1 s before growth stop, but they are actually at the same 53 s from the standpoint of InAs growth time. In such conventional QD growth cases, the initial increase of RHEED intensity versus time is naturally the same, while the final saturation level comes down with decreasing InAs coverage. Using 53 s of InAs deposition, whose coverage equals the critical wetting layer thickness, the RHEED intensity increases immediately following the growth stop and as speed as the above two, but soon saturates at a lower level (not shown). When the InAs deposition time is less than 53 s, i.e., on a subcritical wetting layer, the apparent increase of RHEED intensity is delayed, and this delay is longer and longer as the coverage decreases. At the same time, the increase rate is slowed down, and the final RHEED intensity is lowered. When the InAs coverage is less than 1.60 ML, the RHEED intensity is still increasing after 2 min of postgrowth annealing. In fact, there is certainly a saturation behavior even for lower InAs coverage as long as the postgrowth annealing time is sufficiently long. In Fig. 3(b), the evolutions of RHEED intensity for InAs growth time of 50, 49, and 48 s are presented up to about 5 min of postgrowth annealing, which indicates the trend of RHEED intensity saturation for lower InAs coverage.

The saturation behavior can be used to establish the quantitative correspondence between RHEED intensity and the actual volume of QD's. We use STM, which is more accurate than AFM, to measure the QD volume. A sample with saturated QD's volume is not expected to be subject to changing in QD's volume during the cooling down process mentioned above. Such a cooled sample is then covered by a few micrometers of amorphous arsenic for STM observation.[12] By integrating the STM data using an image processing program, the volume of observed QD's is obtained. As an example, the QD's in Fig. 1(a) have a lateral diameter of 19.5 nm and a height of 2.3 nm in average, and accordingly the saturation RHEED intensity for 54 s of InAs coverage shown in Fig. 3(a) corresponds to a total QD's volume of about 0.18 ML.

Although the evolution of total QD's volume looks similar in two cases of QD formation, that with InAs growth continuing after and stopping before the conventional 2D-3D growth mode transition, they differ in detailed characteristics. It is found that the evolution of RHEED intensity I with postgrowth annealing time t from a subcritical wetting layer can be expressed as

$$I = I_0(1 - e^{-t/\tau}), \tag{1}$$

where I_0 corresponds to the saturation value of RHEED intensity and τ is a time constant. The fitted results are shown by solid curves in Fig. 3. It is clear that the data of RHEED intensity for QD formation from a subcritical wetting layer are well fitted. The aforementioned delay of apparent increase is a result of RHEED intensity below the background before a certain of annealing time. However, those for conventional QD formation are poorly matched. This is easily seen in the region of transition from rapid increase to saturation of RHEED intensity. In detail, if τ is tuned to fit the transition region, it fails in matching the initial rapid increase, and vice versa. It means that QD formation in the atmosphere of InAs deposition flux is somehow different from that without InAs deposition. On the other hand, the result for 54 s of InAs growth is not far from Eq. (1), suggestive of some common mechanism between the cases of coverage below and slightly above the critical thickness. These results remain for different substrate temperatures and different InAs growth rates in our experimental range. Nevertheless, the present study is limited up to 500 °C because a higher substrate temperature leads to a slow decreasing RHEED intensity replacing the saturation behavior, which has been observed before and ascribed to InAs desorption.[9]

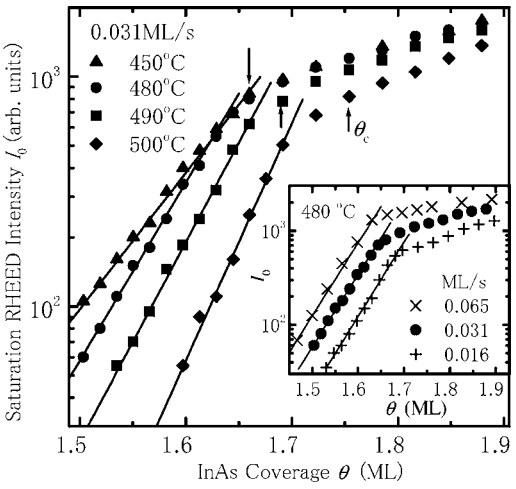

FIG. 4. InAs coverage dependence of the saturation RHEED Intensity I_0 obtained by fitting the RHEED data with Eq. (1) for different substrate temperatures and different InAs growth rates (inset). Arrows indicate the critical thickness θ_c. The straight lines are the exponential fittings of the data well before θ_c by Eq. (2).

The fitted results of the saturation RHEED intensity I_0 are presented in Fig. 4. With increasing coverage of a subcritical InAs wetting layer, I_0 increases exponentially although this dependence does not extend up to the critical thickness θ_c. As the temperature is raised, this exponential variation becomes steeper. Meanwhile, the critical thickness increases, similar to the previous reports.[13] In the region with coverage θ well above θ_c, I_0 changes linearly with θ, although it is displayed on a logarithmic scale. This is in agreement with the previous result that QD volume changes as a linear function of InAs coverage.[14] With different InAs growth rates, the exponential slope for I_0 versus θ does not show obvious change. However, I_0 itself is weakly reduced with lowering InAs growth rate. For $\theta > \theta_c$, this observation coincides with others' observation on conventional QD's growth.[15] One example at substrate temperature of 480 °C can be seen in the inset of Fig. 4.

Figure 5 shows the coverage dependence of fitted τ^{-1}, which describes the speed of QD formation. In the range of coverage θ well below θ_c, τ^{-1} decreases exponentially with decreasing coverage. At low temperatures up to 480 °C, the exponential slope of τ^{-1} versus θ keeps almost unchanged. With temperature further raised, the variation of τ^{-1} with θ

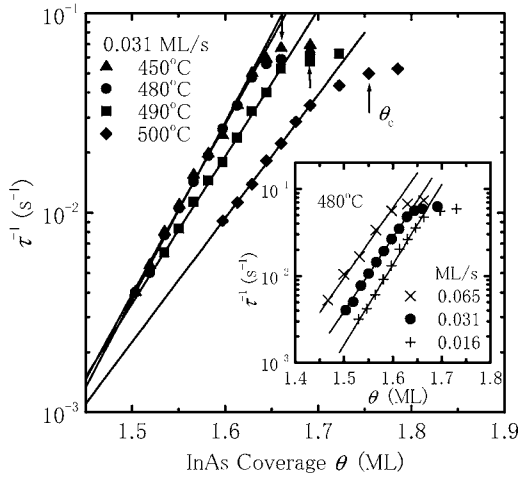

FIG. 5. InAs coverage dependence of τ^{-1} obtained by fitting the RHEED data with Eq. (1) for different substrate temperatures and different InAs growth rates (inset). Arrows indicate the critical thickness θ_c. The straight lines are the exponential fittings of the data well before θ_c by Eq. (2).

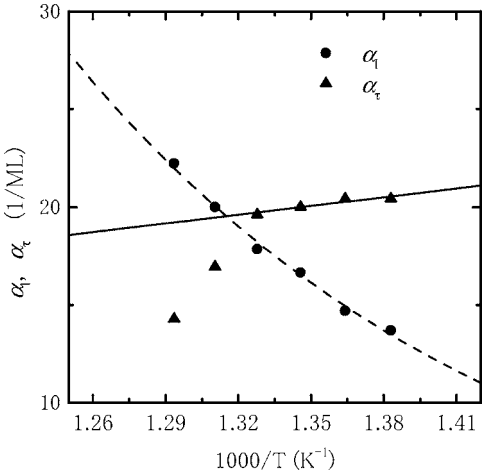

FIG. 6. The exponential slope for the InAs coverage dependence of I_0 and τ^{-1}, obtained by fitting related data in Figs. 4 and 5 with Eq. (2), as a function of substrate temperature T. The dashed curve shows the fitting of α_I, proportional to D, by Eq. (9). The solid line indicates the inverse temperature dependence of α_τ as can be deduced from Eq. (4).

becomes less and less steep, in contrast to that for I_0 versus θ seen in Fig. 4. Since the time evolution of RHEED intensity for θ well above θ_c cannot be well fitted by Eq. (1), the maximum coverage in presenting τ^{-1} is only slightly higher than θ_c. Around θ_c, τ^{-1} deviates down from the exponential coverage dependence and tends to be constant. The τ^{-1} value around θ_c looks invariable at low temperatures but decreases at higher temperatures. On the growth rate dependence, representative results at 480 °C are shown in the inset of Fig. 5. The exponential slope for τ^{-1} versus θ are almost independent of the InAs deposition rate. With decreasing InAs growth rate, τ^{-1} value around θ_c does not change much, although is weakly degrading.

Fitting the above observed coverage dependence of τ^{-1} and I_0 in the subcritical regimes with

$$I_0 \propto e^{\alpha_I \theta},$$

$$\tau^{-1} \propto e^{\alpha_\tau \theta}, \tag{2}$$

as indicated by solid lines in Fig. 4 and 5, we have exponential slope α displayed by scattered symbols as a function of temperature T as shown in Fig. 6. It intuitively presents the different behaviors of I_0 and τ^{-1}, indicative of different decisive factors in their variations.

The above observations illustrate QD formation from a subcritical InAs wetting layer by postgrowth annealing. Although RHEED does not show any change from 2D growth of the wetting layer before QD formation, the different results for different InAs coverage imply something progresses with the growth of wetting layer. It is then important to examine what happen on this "flat" surface before QD formation. The morphology at the point of growth stop needs to freeze, but it has been found difficult to see the real surface of such a strained layer due to unavoidable effects of annealing.[8] Here we use an indirect method. After growth stop, the InAs wetting layer is immediately capped by GaAs at a high growth rate of 2 ML/s for less than 2 min without increasing the growth temperature, which produces an InAs/GaAs quantum well structure, followed by soon cooling down the sample in the way mentioned for QD's. We measured the photoluminescence (PL) of such quantum wells at 77 K with excitation of the 514.5 nm line of a Ar^+ laser. The PL spectra are presented in Fig. 7. We see that, with increasing well width, the PL peak of the InAs/GaAs quantum well broadens. With well width of 1.64 ML, which is the nearest to the critical thickness, the peak of the quantum well is superimposed on the tail of a broad peak, indicating the existence of a RHEED-undetectable number of InAs QD's. The change of the inhomogeneous broadening implies that the fluctuation of the effective quantum well width increases with the nominal well width. Of course, the

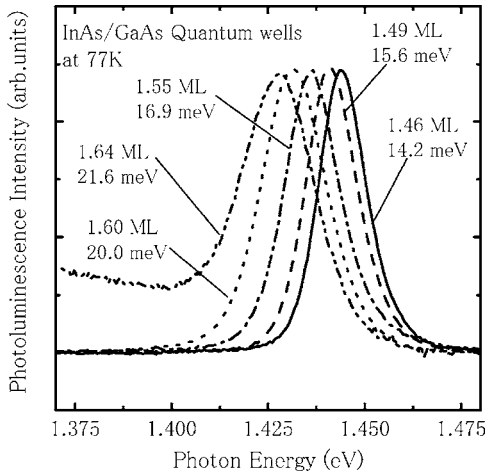

FIG. 7. PL spectra of InAs/GaAs quantum wells, which were fabricated with rapidly depositing GaAs capping layer immediately after the InAs deposition. The numbers denote the nominal well width and the full width at maximum of the spectra.

overgrown interface does not definitely represent the morphology of as-grown wetting layer surface. Some effect such as Indium segregation into GaAs cap layer during overgrowth may also induce PL broadening. However, such an effect is suppressed in our samples by quick capping and rapid cooling. In addition, the monotonic increase in the PL peak width with wetting layer thickness is different from the absence of clear well width dependence of an indium-segregation-induced PL broadness for InGaAs/GaAs quantum wells.[16] In contrast, an indium-segregation-induced narrower PL peak of InAs/GaAs quantum wells has ever been observed.[17] Even if the indium segregation is playing some role in PL broadening in our samples, it might be associated with the roughness of as-grown surface, because indium segregation is found to prefer the top of islands.[18] Therefore, our PL study on differently thick InAs/GaAs quantum wells suggests to a high degree that the InAs wetting layer before 2D-3D growth mode transition is rougher and rougher with growing time. This is correlated with the coverage dependence of total QD's volume as observed above, and may serve as the base to understand the QD formation mechanisms.

III. DISCUSSION

Surface roughening in epitaxial growth has received much attention in recent years.[19] On the 2D strained InAs wetting layer, it was found that the surface becomes much rougher even with slightly increasing the InAs coverage from 1.3 to 1.4 ML.[20] In some cases, small 3D islands can be formed from such an InAs wetting layer.[7] Our PL results in Fig. 7 provide evidence of similar phenomenon in our samples. Theoretical studies show that, due to the existence of roughness, a 2D stained film is always unstable,[21,22] and nucleation can occur to form 3D islands as long as the initial surface is sufficiently rough.[5] On the other hand, self-assembled QD's are widely regarded as arising from precursors, including some floating features,[20] 2D platelets,[23,24] and quasi-3D islands.[25] The floating features and 2D platelets may locate on the top of large 2D islands. This causes locally one monolayer fluctuation of the wetting layer thickness. Quasi-3D islands sitting on the 2D flat wetting layer are a couple of monolayers high so that it gives rise to larger roughness of the wetting layer than 2D platelets do. Therefore, we ascribe the observed roughness of an as-grown wetting layer to, at least partly, the existence of precursors for QD's formation in our samples. In the following, we shall analyze our observations in view of QD formation through transformation of precursors formed during InAs deposition.

A. Rate equations

Considering mass transport between adatoms, 2D precursors and 3D QD's, Dobbs *et al.* advanced a mean-field theory on self-assembled QD's.[26] They started their calculation from the beginning of conventional QD formation. We extend the analysis to the stage well before 2D-3D growth mode transition. Then the 2D growth of the wetting layer has to be taken into account. As an approximation, we regard it as the attachment of adatoms to the pure 2D wetting layer with an attachment rate β. As to the precursors, we consider 2D platelets and quasi-3D islands sitting above the pure 2D wetting layer as just mentioned. In our samples, quasi-3D islands may be the main precursors or more realistic due to the obvious roughness of the wetting layer. In addition, 2D platelets can rearrange into bilayer, trilayer islands,[27] suggesting a precursor conversion from 2D to quasi-3D islands, so that we may treat the precursors as one type. Conversion of a precursor by migration of the peripheral atoms to its top gives rise to the formation of a QD on the top of a wetting layer,[26] which is described by a nucleation rate γ. All of these pure 2D wetting layers, precursors, and QD's are capturing adatoms, which are supplied by InAs deposition and are distributed on the top of the whole surface, including that of pure 2D wetting layers, precursors, and QD's. Based on the mean-field theory of Ref. 26, we are able to deal with the amounts, meaning the product of size and density, of adatoms n_1, precursors n_2, and QD's n_3, in terms of atom numbers or equivalently volumes in unit of ML. The rate equations are thus written as

$$\frac{dn_1}{dt} = F - \beta n_1 - D(\sigma_2 n_2 + \sigma_3 n_3) n_1,$$

$$\frac{dn_2}{dt} = D\sigma_2 n_1 n_2 - \gamma n_2,$$

$$\frac{dn_3}{dt} = D\sigma_3 n_1 n_3 + \gamma n_2, \tag{3}$$

where F is the InAs deposition rate, D is the diffusion coefficient of adatoms, σ_2 and σ_3 are the normalized capture number for adatoms to be captured by the precursors and QD's, respectively. Here we do not include exact analysis of the precursors with critical size since they are normally much less than the total ones. Instead, we set an initial value of n_2 to replace the starting role of critically sized precursors. We also neglect the contribution of an adatom escaping from the precursors because it has only a minor quantitative effect. Using this equation, one can simulate the QD formation and study the evolution of precursors.

B. Time evolution

Before simulating the QD formation, some parameters have to be further considered. In the rate equations, the attachment rate β is in principle affected by the surface geometry. It is expected to decay as the precursors and QD's increases because the effective pure 2D flat area is decreased. We take a form of $\beta = \beta_0(1 - s_2 - s_3)$, where s_2 and s_3 are the base areas of the precursors and QD's, respectively, estimated by modeling them as cone shaped. The precursors are taken to be 3 ML high for calculation of s_2 and the averaged STM data of saturated QD's are used for calculation of s_3. Although this is not exact owing to the changing height with time, especially in the beginning, it is found that this treatment gives a difference less than 10% from that using a constant $\beta = \beta_0$ and those using linearly changing heights.

The capture numbers are usually complex functions of the size and shape of precursors and QD's. From Ref. 26, one may expect the capture number to be a roughly increasing function of the size. In our rate equations dealing with the amount, not the density, the normalized capture number σ_2 and σ_3 is in fact the ratio of the capture number of each precursor or QD to the size. As an approximate result, we regard the normalized capture numbers as a constant parameter. QD nucleation rate γ is thermally activated[24] with activation energy being QD formation energy. It is also considered exponentially depending on the so-called superstress of the wetting layer, $(\theta-\theta_c)/\theta_c$, via QD formation energy.[4] Taking these two aspects into account, we may have

$$\gamma = \gamma_0 \exp\left(-\frac{\theta_c-\theta}{\theta_c}\frac{E}{k_BT}\right) \tag{4}$$

with constants γ_0 and E. The term $E(\theta_c-\theta)/\theta_c$ plays the role of QD formation energy, whose coverage dependence might be comprehended by the change of the precursors, e.g., higher and/or larger quasi-3D islands at higher coverage.[4,27] On a growing 2D strained film such as a wetting layer, it has been proposed that some mechanisms such as long-range van der Waals forces[28] or nonlinear elastic effects[5] act to stabilize the system, in other words, to suppress the formation of QD's as usually observed. These effects can be reflected by a QD formation energy coefficient E increasing with the growth rate F. The exact form of E as a function of F is still unknown but we found that setting it to be 12, 10 and 8 times that of $F=0$ for the presently used InAs growth rates 0.065, 0.031, and 0.016 ML/s, respectively, give the best simulation.

To set the initial conditions for QD formation, we consider that the pure 2D wetting layer and adatoms are in dynamic equilibrium before the appearance of precursors, i.e., $dn_1/dt=F-\beta n_1=0$ before n_2 starts to grow. The growth of pure 2D wetting layer usually proceeds in a way of forming large 2D islands. The precursors start to grow probably when the interaction of those large 2D islands occurs from about 1.4 ML of coverage.[23] Accordingly, we set initial n_2 to be a finite small value around 1.4 ML. At the same temperature and growth rate, results for different InAs coverage are obtained by changing the growth time using Eq. (3) and (4). In Fig. 3, the dashed curves show the simulation results at 480 °C and 0.031 ML/s. It is seen that Eq. (3) well describes the QD formation process both for conventional QD growth and for postgrowth annealing of a subcritical wetting layer.

For the QD formation from a subcritical wetting layer, the matching between the simulation according to Eq. (3) and the fitting according to Eq. (1) can be understood as follows. As the InAs wetting layer is growing before 2D–3D transition, the adatoms firstly decrease very slowly but gradually faster and the precursors increase rapidly, as shown by the thick dotted and dashed lines in Fig. 8. In the meantime, the QD nucleation rate is negligible due to large superstress and very high QD formation energy, as suggested by Eq. (4). As a result, the amount of QD's is too low to have a visible effect, as can be expected from the thick solid lines shown in Fig. 8. It is implied that precursors are formed by consuming adatoms but without converting into QD's as the wetting layer is growing. If the QD formation after growth stop of a wetting layer is further excluded by setting $\gamma=0$, it is seen that n_1 decreases steeply and n_2 saturates immediately, as shown by the thin solid lines in Fig. 8. This result enables a simplified treatment of QD formation from a subcritical wetting layer. We can approximately take $n_1=0$ and n_2 being the saturation value, n_2^s, as the initial conditions for QD formation at $F=0$. Once InAs deposition is stopped, the precursors are allowed to convert into QD's because the QD nucleation rate γ is changed from ignorable to finite due to the decrease of QD formation energy. The rate equations can thus be written as

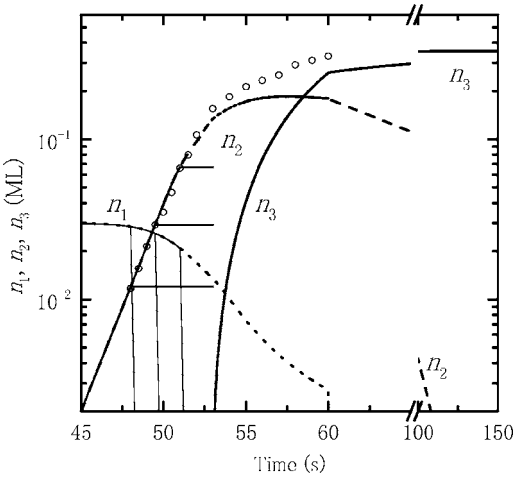

FIG. 8. Thick curves: time dependence of the amount of adatoms n_1, precursors n_2, and QD's n_3 simulated by using Eqs. (3) and (4) for 60 s of InAs deposition at growth rate of 0.031 ML/s. Thinner solid curves: the effect of InAs growth stop before 2D-3D transition without considering QD's. The parameter values and initial conditions are the same as those in Fig. 3. Scattered circles show measured saturation QD's volume for different InAs growth time.

$$\frac{dn_2}{dt} = -\gamma n_2,$$

$$\frac{dn_3}{dt} = \gamma n_2. \tag{5}$$

With a constant γ, which is nearly the case for InAs growth stop before conventional 2D-3D transition, it is straight to have

$$n_3 = n_2^s(1-e^{-\gamma t}), \tag{6}$$

which is the same as Eq. (1). This explains the nearly identical curves simulated by Eq. (3) and fitted to Eq. (1). What is more important, it indicates that QD's nucleation in postgrowth annealing of a subcritical wetting layer is the conversion of precursors emerging before growth stop into QD's.

To analyze the conventional QD formation with InAs deposition, it is also useful to see the effect of adatoms and precursors. We note that the simulation is good with $\sigma_3=2\sigma_2$ but poor with $\sigma_3=0$. It means that conventional QD

formation does involve direct consumption of adatoms and may explain the mismatching of experimental RHEED intensity to Eq. (1). Although the adatoms are always decreasing, as shown by the dotted line in Fig. 8, their direct attachment to QD's is enhancing due to the rapidly increasing QD's volume after 2D-3D transition. On the other hand, QD nucleation from precursors are also important, as can be seen by comparing n_2 and n_3 for InAs growth of 60 s shown in Fig. 8. In the final total QD's volume of 0.37 ML, that from InAs supplying after 2D-3D transition is about 0.22 ML. The rest 0.15 ML is often termed mass transport from the wetting layer.[27] At the critical point of 53 s, n_2 increases to be about 0.15 ML. It is clear that, in our observation range, the often observed mass transport from the wetting layer during QD's formation can be interpreted by the existence of precursors, which is a part of the entire wetting layer as has been considered,[4] before conventional 2D-3D transition. After 2D-3D transition, the precursors continue forming by capturing adatoms and at the same time converting to QD's. As the growth stops, the adatoms soon disappear and only the precursors are supplying QD's with materials until they run out, when the QD's volume saturates. Therefore, precursors play an important role in QD formation.

C. Saturation QD's volume

In Fig. 8, the scattered symbols show the saturation QD's volume, which is obtained by calibrating the saturation RHEED intensity to the data measured by STM. Its agreement with the simulated saturation level of n_3 has been shown in Fig. 3 and can be seen here by comparing to the saturation level of the thick solid line. In the case of postgrowth annealing of a subcritical wetting layer, the saturation QD's volume follows n_2^s in Eq. (6), so that its consistent behavior with n_2 shown here is natural. More importantly, the exponential coverage dependence of the saturation QD's volume seen in Fig. 4 can be understood using the present model. As has been mentioned, QD's can be ignored during the growth of a wetting layer. Consequently, the rate equations for a subcritical wetting layer can be simplified as

$$\frac{dn_1}{dt} = F - \beta n_1 - D\sigma_2 n_2 n_1,$$

$$\frac{dn_2}{dt} = D\sigma_2 n_1 n_2. \tag{7}$$

Since the early n_1 changes little and n_2 is initially small, then $dn_2/dt \approx D\sigma_2 F\beta^{-1} n_2$ at the early stage of precursors formation. Approximately it reads the exponential increase of precursors

$$n_2 \propto e^{D\sigma_2\beta^{-1}Ft} = e^{D\sigma_2\beta^{-1}\theta}, \tag{8}$$

which explains the exponential coverage dependence of the saturation QD's volume I_0 seen in Fig. 4. Comparing Eq. (8) to Eq. (2), the exponential slope α_I is proportional to[29]

$$D = \frac{k_B T}{h} e^{-E_s/k_B T}, \tag{9}$$

where E_s is an energy barrier for adatoms to hopping between surface sites, k_B is the Boltzman constant, and h is the Planck constant. This relation interprets the temperature dependent slope for the exponential I_0 variation with θ seen in Fig. 4, because α_I in Fig. 6 can be well fitted by Eq. (9) as shown by the dashed line. This fitting gives an energy barrier E_s of 0.47 eV. It is somehow different from the values used in previous theories, 1.04 eV[25] and 0.69 eV (8000 K),[4] probably due to the temperature dependence of the capture number σ_2 and attachment rate β, which have to be taken into account for a more precise treatment. Meanwhile, no apparent growth rate dependence of α_I can be seen from Eqs. (8) and (9). This is consistent with our observation as shown in the inset of Fig. 4.

D. QD nucleation rate

Comparing Eq. (1) with (6), the QD nucleation rate γ is equivalent to τ^{-1}. Based on Eq. (4), the exponential increase of τ^{-1} versus θ shown in Fig. 5 is understood as the superstress dependence of the QD formation energy. Equation (4) implies that the exponential slope of τ^{-1} versus θ, α_τ, should be inversely proportional to T. As shown by the solid line in Fig. 6, α_τ values up to 480 °C satisfy this relation. From this comparison, we obtain $E=2.0\pm0.3$ eV and further deduce $\gamma_0=0.09\pm0.02$ s^{-1}, which are in agreement with the values used in the above simulations. Note that E is not the QD formation energy. Taking the superstress into account, the QD formation energy $E(\theta_c-\theta)/\theta_c$ at the presently observed lowest coverage is about 0.2 and 2.0 eV for QD formation by postgrowth annealing of a subcritical wetting layer and in the conventional case, respectively. However, severe deviation from Eq. (4) occurs at higher temperatures in Fig. 6. This is probably caused by the change in QD formation energy due to possible InAs desorption, which is open to further study. In addition, Eq. (4) suggests that α_τ might be growth rate independent as observed in the inset of Fig. 5.

In the case of conventional QD formation with InAs deposition, nucleation rate γ is not so constant but in average close to γ_0 because, at the early stage of QD formation, whose nucleation rate is decisive, the superstress is near 0. Around the critical point, the difference of γ between different growth rates becomes small according to Eq. (9). This is the reason why the experimental τ^{-1} for a near critical wetting layer is not so different from the value for $\theta > \theta_c$, and it explains the observed almost growth rate independent τ^{-1} for θ around θ_c seen in the inset of Fig. 5.

IV. SUMMARY

In summary, we studied InAs/GaAs QD's formation by postgrowth annealing of a wetting layer thinner than the critical thickness for 2D-3D growth mode transition. RHEED is found a powerful tool to quantitatively investigate QD formation in this case. With postgrowth annealing time, the total QD's volume initially increases and finally satu-

rates, which is well explained by precursors growing during wetting layer deposition and transforming into nucleated QD's after deposition stop, on the basis of a mean-field theory. Both of the saturation QD's volume and the QD nucleation rate depend exponentially on the InAs coverage. The former shows a thermally activated slope, which follows the diffusion of adatoms to precursors. The latter is considered resulting from exponential superstress dependence of the QD formation energy. Consistently, the above exponential slopes are almost independent of the wetting layer growth rate. In conventional InAs/GaAs QD growth, the precursors emerging before 2D-3D transition are suggested to be responsible for the usually observed mass transport from wetting layer to QD's.

[1] D. Bimberg, M. Grundmann, and N. Ledentsov, *Quantum Dot Heterostructures* (Wiley, Chichester, 1998).
[2] D. E. Jesson, T. P. Munt, V. A. Shchukin, and D. Bimberg, Phys. Rev. Lett. **92**, 115503 (2004).
[3] F. Patella, S. Nufris, F. Arciprete, M. Fanfoni, E. Placidi, A. Sgarlata, and A. Balzarotti, Phys. Rev. B **67**, 205308(R) (2003).
[4] V. G. Dubrovskii, G. E. Cirlin, and V. M. Ustinov, Phys. Rev. B **68**, 075409 (2003).
[5] H. R. Eisenberg and D. Kandel, Phys. Rev. Lett. **85**, 1286 (2000).
[6] K. M. Chen, D. E. Jesson, S. J. Pennycook, T. Thundat, and R. J. Warmack, Phys. Rev. B **56**, R1700 (1997).
[7] A. Polimeni, A. Patanè, M. Capizzi, F. Martelli, L. Nasi, and G. Salviati, Phys. Rev. B **53**, R4213 (1996).
[8] T. J. Krzyzewski and T. S. Jones, J. Appl. Phys. **96**, 668 (2004).
[9] Ch. Heyn, Phys. Rev. B **66**, 075307(R) (2002).
[10] P. Finnie, B. J. Riel, and Z. R. Wasilewski, J. Vac. Sci. Technol. B **20**, 2210 (2002).
[11] N. Saucedo-Zeni, A. Yu. Gorbatchev, and V. H. Méndez-García, J. Vac. Sci. Technol. B **22**, 1503 (2004).
[12] H. Z. Song, M. Kawabe, Y. Okada, Y. Yoshizaki, T. Usuki, N. Nakata, T. Ohshima, and N. Yokoyama, Appl. Phys. Lett. **85**, 2355 (2004).
[13] P. B. Joyce, T. J. Krzyzewski, G. R. Bell, B. A. Joyce, and T. S. Jones, Phys. Rev. B **58**, R15981 (1998).
[14] T. J. Krzyzewski, P. B. Joyce, G. R. Bell, and T. S. Jones, Phys. Rev. B **66**, 201302(R) (2002).
[15] P. B. Joyce, T. J. Krzyzewski, G. R. Bell, T. S. Jones, S. Malik, D. Childs, and R. Murray, Phys. Rev. B **62**, R10891 (2000).
[16] C. M. Yee-Rend'on, M. L'opez-L'opez, and M. Mel'endez-Lira, Rev. Mex. Fis. **50**, 193 (2004).
[17] K. Yamaguchi, Y. Yasuda, A. Kova'cs, and P. B. Barna, J. Appl. Phys. **89**, 217 (2001).
[18] N. Grandjean, J. Massies, and O. Tottereau, Phys. Rev. B **55**, R10189 (1997).
[19] J. M. López, M. Castro, and R. Gallego, Phys. Rev. Lett. **94**, 166103 (2005).
[20] F. Patella, S. Nufris, F. Arciprete, M. Fanfoni, E. Placidi, A. Sgarlata, and A. Balzarotti, Phys. Rev. B **67**, 205308(R) (2003).
[21] B. J. Spencer, P. W. Voorhees, and S. H. Davis, Phys. Rev. Lett. **67**, 3696 (1991).
[22] F. Long, S. P. A. Gill, and A. C. F. Cocks, Phys. Rev. B **64**, 121307(R) (2001).
[23] C. Priester and M. Lannoo, Phys. Rev. Lett. **75**, 93 (1995).
[24] Y. Chen and J. Washburn, Phys. Rev. Lett. **77**, 4046 (1996).
[25] T. J. Krzyzewski, P. B. Joyce, G. R. Bell, and T. S. Jones, Phys. Rev. B **66**, 121307(R) (2002).
[26] H. T. Dobbs, D. D. Vvedensky, A. Zangwill, J. Johansson, N. Carlsson, and W. Seifert, Phys. Rev. Lett. **79**, 897 (1997).
[27] E. Korutcheva, A. M. Turiel, and I. Markov, Phys. Rev. B **61**, 16890 (2000).
[28] D. Leonard, K. Pond, and P. M. Petroff, Phys. Rev. B **50**, 11687 (1994).
[29] S. Suo and Z. Zhang, Phys. Rev. B **58**, 5116 (1998).